3D in SEM, (S)TEM, Ion Imaging, incl. FIB-SEM and SBF-SEM

MIM.1.P015
Practical Aspects of 3D Crystalline Defect Analysis for Engineering Materials using Scanning Transmission Electron Microscopy

L. Agudo Jácome[1,2]

[1]Bundesanstalt für Materialforschung und -prüfung, Abteilung für Werkstofftechnik, Berlin, Germany
[2] Ruhr-Universität Bochum, Institut für Werkstoffe, Bochum, Germany

leonardo.agudo@bam.de
Keywords: dislocations, scanning transmission electron microscopy (STEM), high angle annular darkfield detector (HAADF), stereography

Structural and functional engineering materials under thermal, mechanical or thermomechanical service conditions suffer from microstructural degradation which is due to crystalline defects such as dislocations. Since the introduction of the transmission electron microscope (TEM), diffraction contrast has been implemented in conventional (C)TEM to image and analyze crystalline defects, based on the effect of the displacement vector R, characteristic for crystalline defects. Nevertheless, when applying diffraction contrast in conventional (C)TEM by setting proper two-beam conditions, the presence of strong phase contrast artefacts such as bending, thickness and extinction contours often hinders proper observation of highly defected material volumes. Although already in the 1970s it was proven that diffraction contrast using scanning (S)TEM helps eliminating these artefacts [1-3], only in the past few years STEM has started to gain intensive application in this field, thanks to the accessibility of field emission gun (FEG) TEMs and the development of more efficient STEM detectors. These allow for an increased signal-to-noise ratio (comparable to CTEM imaging) and larger and more flexible divergence angle tolerances. Thus, interest in STEM diffraction contrast imaging has been increasing in recent years in the field of defect analysis [4-6]. At the EC2009, a first approach on using multibeam contrast and stereomicrocopy in STEM mode to facilitate quantitative evaluation of three-dimensional (3D) dislocation structures was introduced [7]. In the present contribution practical aspects to be considered when applying the aforementioned TEM techniques, e.g., the effect of camera length, of the depth of focus and of surface effects on STEM stereomicroscopy are discussed. Finally differences arising from using different microscopes with similar equipment are highlighted.

The applicability of STEM stereo-imaging is mostly shown here on TEM-foils of a single crystalline Ni-based superalloy subjected to creep deformation. Under creep conditions, dislocations in different regions of the microstructure, i. e., in the matrix phase (γ), in the ordered precipitate (γ') and between γ/γ' interfaces. The effect of surface damage on 3D appearance in stereograms is shown by preparing the electron transparent TEM foils by different conventional techniques. TEM was performed on two analytical FEG-TEMs with similar characteristics operating at 200kV: a TECNAI F20 S-Twin and a Jeol 2200FS. STEM images were acquired with the high angle annular dark field (HAADF) detector in both TEMs with optimized illumination conditions.

By acquiring a diffraction contrast stereo-pair in STEM, the absence of bending contours, thickness contours and extinction contours enables a clear 3D impression of regions of up to 40 μm^2. In Figure 1, three material examples are provided, which demonstrate this possibility. Another particular feature of STEM imaging has to do with the depth of field, which is considerably reduced compared to CTEM at a similar magnification. To illustrate the consequence of a reduced depth o field, Figure 2a shows a stereogram that appears focused only in its central region. The depth of field in this case is of ~250 nm and the TEM foil has a similar thickness at the imaged region. Nevertheless, in order to obtain the two-beam condition for both micrographs of the stereogram, the sample had to be tilted strongly by using both the eucentric tilt axis and its orthogonal tilt axis. Consequently, if one focuses the center of the image for both tilt positions of the stereogram, the inclination of the specimen will cause an increasing defocus towards the sides of each of the micrographs of the stereogram, leading to the blurred appearance outside the central area of Figure 2a. Nevertheless, this effect may be corrected by simultaneously varying the focus height while each of the images of the stereogram is acquired, resulting in a stereogram such as that in Figure 2b.

1. D.M. Maher and D.C. Joy, Ultramicoscopy 1 (1976) p. 239.
2. C.J. Humphreys, Ultramicroscopy 7 (1981) p. 7
3. T. Yamamoto and H. Nishizawa, Physica Status Solidi A 28 (1975) p. 237.
4. J. Pešička, A. Aghajani, Ch. Somsen, A. Hartmaier and G. Eggeler, Scr. Mater. 62 (2010) p. 353.
5. P.J. Phillips, M.C.Brandes, M.J. Mills and M. DeGraef, Ultramicroscopy 111 (2011) p. 1483.
6. L. Agudo Jácome, G. Eggeler, A. Dlouhý, Ultramicroscopy 122 (2012) p. 48.
7. L. Agudo Jácome, Ch. Somsen, and G. Eggeler, in MC2009, eds. W. Grogger, F. Hofer and P. Pölt, (Verlag der TU Graz, Graz) (2009), p. 201.

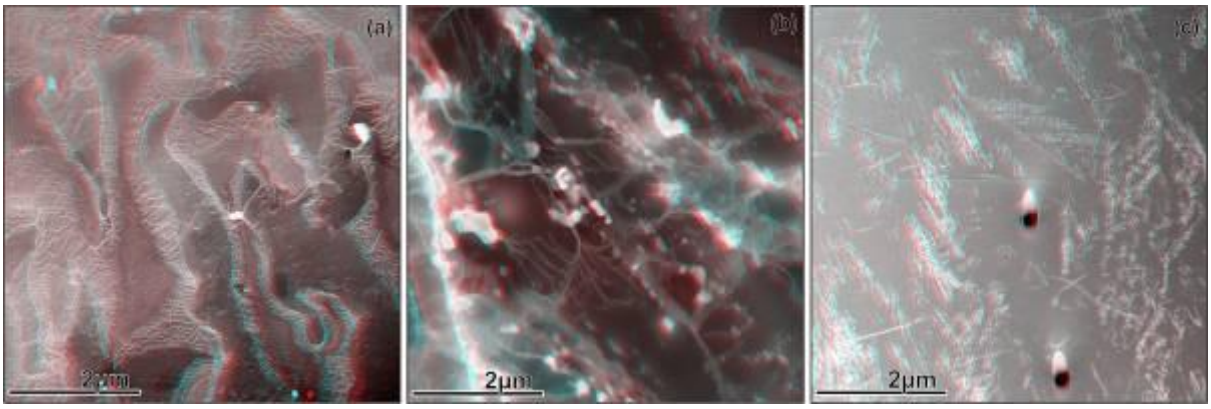

Figure 1. 3D stereograms of the microstructures of (a) a single crystal Ni-base super alloy after creep. **g** = (111), (b) a tempered martensite ferritic steel after creep. **g** = (200), (c) the B2 phase (austenite) of a NiTi shape memory alloy after 5 transformation cycles; **g** = (200)..

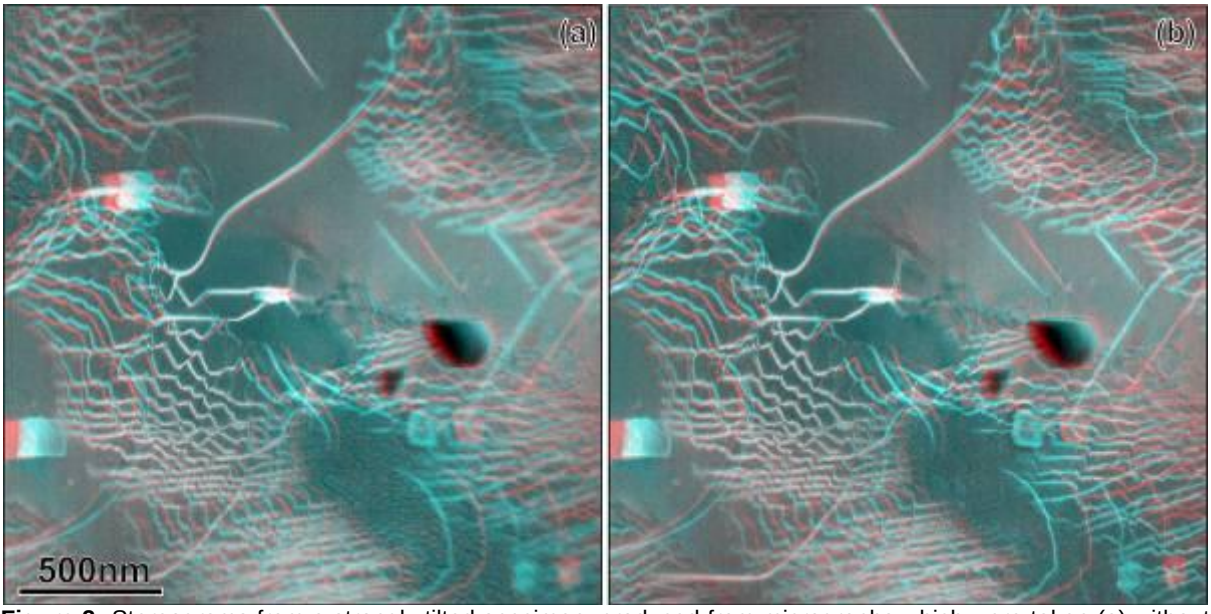

Figure 2. Stereograms from a strongly tilted specimen, produced from micrographs which were taken (a) without focus correction and (b) with dynamic focus correction. **g** = (111)..